Analysis of Circularly Polarized Light Irradiation Effects on Double Ferromagnetic-Gate Silicene Junction

Peerasak Chantngarm[1] and **Kou Yamada**[2]

ABSTRACT

We present an analytical study of effects that off-resonant circularly polarized light irradiation has on spin-valley currents in dual ferromagnetic-gate silicene-based junctions. Two identical electric fields are applied to both ferromagnetic (FM) gates. Two types of exchange field configurations, parallel (P) and anti-parallel (AP), are applied along with chemical potential to the FM gates in this investigation. The results show that application of circularly polarized light has an impact on polarized spin and valley current characteristics, particularly at the off-resonant frequency region. It also enhances the amplitude of tunnelling magnetoresistance (TMR) significantly. In addition, we found that exchange field configuration has an effect on both spin polarization and valley polarization. Our study reveals that light intensity plays the main role on the light irradiation effects, where the band structure and change electronic properties of the materials are modified by photon dressing to create a new phase of electronic structure. The change of band structure in each region affects the transmission coefficients and transmission probability amplitude of electrons, which in turn affects the conductance of each spin-valley current component. Our study suggests the potential of this scheme in applications, such as spin-valleytronic photo-sensing devices under polarized-photo irradiation.

Keywords: Silicene, Spin-Valleytronics, Photo-Sensing Devices

1. INTRODUCTION

Silicene has recently attracted much attention after experimental evidence [1]. It is considered to be a candidate for the post-bulk-silicon era along with other artificial elemental 2D materials such as graphene (C), germanene (Ge), Borophene (B), phosphorene (P), stanene (Sn) and plumbene (Pb) in electronics, spintronics, valleytronics and quantum computing applications. Among these elemental 2D materials, silicene is currently considered to be the most promising candidate mainly due to the accumulation of silicon-related technology and knowhow in semiconductor industry. Although silicene is a zero-bandgap semiconductor with a small band gap of 1.55 meV in theory, the buckled honeycomb lattice structure allows Dirac electron mass and its band structure to be manipulated easily by electric field [2], which is important in making electronics devices. The honeycomb lattice structure of silicene results in the existence of two atoms in one unit cell, and gives rise to two sublattices, A and B. This two-sublattice system contributes to a new concept called pseudospin. The two-dimensional buckled honeycomb lattice structure in silicene causes tuneable spin-valley coupled band structure and gives rise to topological phase transition, an intriguing transport phenomenon.

There have been many theoretical and computational studies in spin- and valley-polarized transport in silicene junctions, which helps the progress in this area. The topics of study are, for instance, the mechanism of magnetism that opens different spin-dependent band gaps at k and k' points and results in spin and valley polarized transports [3], the conditions of electric field for the fully valley and spin polarized transports [4], and ballistic transport through silicene ferromagnetic junctions under the presence of magnetic exchange field and normal electric field [5]. Another research area that has been very active is electronic transport of spintronic and valleytronic devices based on silicene, such as spin filter and spin-valley filter [6-8], as well as spin-polarized transport in a dual-gated silicene system where there is no exchange field [9]. Double ferromagnetic-gated silicone-based junction was also recently proposed to control lattice-pseudospin current along with pure spin- and valley-polarized current in silicene giving a possibility for applications in pseudospintronics [10]. The promising electronic properties of silicene has led to more experimental investigations and succeeded in making silicene field-effect transistors (FET) operating at room temperature [11].

Another area that attracts attention more recently is photo-induced effects, similarly to the study in

Manuscript received on August 10, 2017 ; revised on January 25, 2018.

Final manuscript received on January 25, 2018.

[1] The author is with Department of Electronics and Telecommunication Engineering, Faculty of Engineering, Rajamangala University of Technology Krungthep, Bangkok, Thailand., E-mail: cpeerasak@yahoo.com

[2] The author is with Domain of Mechanical Science and Technology, Graduate School of Science and Technology, Gunma University, Gunma, Japan., E-mail: yamada@gunma-u.ac.jp

graphene, where circularly polarized light is used to open a gap at the Dirac point [12]. By irradiation of circularly polarized light at fixed electric field, the topological class of silicene could be changed from quantum spin-Hall insulator (QSHI) to other phase which has different properties [13]. Light irradiation on silicene has effects on the band structure due to photon dressing effect. It is reported that spin- and valley-polarization depends on the intensity of off-resonant circularly polarized light as well as electric field, and it can be inverted by reversing the direction of electric field or the circular polarization of the light [14]. It is found that spin-valley polarizations and tunnelling magnetoresistance in a ferromagnetic-normal-ferromagnetic (FNF) junction can be significantly enhanced by irradiation of off-resonant circularly polarized light on one of ferromagnetic gates without electric field or magnetic field [15]. There is also a study in spin-valley filtering and giant magnetoresistance (GMR) under the photo irradiation in off-resonant frequency region, with which can be applied to photo-sensing devices [16].

In this paper, we study the tight-binding model of silicene-based NM/FM/NM/FM/NM junction under the effects of off-resonant circularly polarized light at the NM region between two FM gates, where NM is normal silicene and FM is ferromagnetic silicene. Two different exchange field configurations, parallel (P) and anti-parallel (AP), are also applied to see the effects. We particularly investigate the effects of photo irradiation on spin- and valley-polarized conductance and tunnelling magnetoresistance (TMR) in this junction. It is found that photo irradiation have significant impact on spin polarization (SP), valley polarization (VP), as well as TMR.

2. MODEL

In this section we explain the structure of double ferromagnetic-gated silicone-based junction in subsection 2.1 and the low-energy effective Hamiltonians based on tight-binding model in subsection 2.2.

2.1 Device Structure

The ballistic transport of electrons in a double ferromagnetic-gated silicene-based structure under external influences as illustrated in Fig. 1 was studied. The numbers following NM and FM in the figure, as in NM1 and FM1, are designated as the identification for each region. Each of the ferromagnetic gates has length LG, and they are apart from each other by distance L. The magnetic exchange energies are designated as h_{1A} and h_{1B} for sublattice-A and sublattice-B at barrier FM1, while their counterparts are designated as h_{2A} and h_{2B} at barrier FM2.

Like the proposal for graphene, silicene might be induced to FM by magnetic insulators EuO due to proximity-induced exchange splitting [17]. A controllable perpendicular electric field E_z is applied to

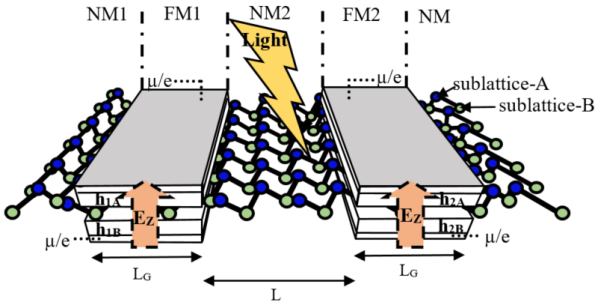

Fig.1: *Cross-sectional schematic model of double-barrier silicene-based NM1/FM1/NM2/FM2/NM3 structure.*

the ferromagnetic barriers FMs. Gate potential μ/e is applied from the top and the bottom of ferromagnetic barriers. Circularly polarized light $A(t) = A_0(\sin(\Omega t), \cos(\Omega t))$ is irradiated to the NM2 region between ferromagnetic gates, where Ω is light frequency, A_t is time-dependent vector potential, and A_0 is the magnitude of light. Circularly polarized light has the planes of the electric field vectors and magnetic field vectors rotate. It has a constant magnitude of electric field while rotating at a steady rate in a plane perpendicular to the direction of the light. Comparing to linearly polarized light, the circularly polarized light has the intensity equivalent in all directions. The off-resonant light frequency used in this study is the frequency region where the electron band structures are changed by virtual photon absorption processes without direct electrons excitation. Light irradiation with off-resonant frequency causes no depumping on optically pumped specimens, and causes no attenuation [18]. In off-resonant frequency scheme, the linear optical process occurs. This means that the amount of light transmitted through a matter is proportional to the irradiated light intensity [19].

2.2 Tight-Binding Hamiltonians

In tight-binding model, the off-resonant light frequency can be achieved when $h|\Omega| \gg t_0$, where h is the Planck constant and t_0 is the nearest hopping energy. The lowest frequency Ω to satisfy this condition can be calculated from the bandwidth 3_{t_0} = 4.8 eV = 10^{15} Hz [13]. The perpendicular distance between the two sublattices due to the buckling structure is 2D = 0.46 Å, where D = 0.23 Å[20]. In this study, we investigate two the electronic transport in two exchange field configurations, parallel junction (P) and anti-parallel junction (AP). The direction of the exchange fields are in this study is assumed to be in-plane with positive sign means right-direction, and negative sign means left-direction. The parallel junction (P) and anti-parallel junctions (AP) are defined as the following exchange field configuration.

P junction : $h_{1A} = h_{1B} = h_{2A} = h_{2B} = 5$ meV,

AP junction : $-h_{1A} = h_{1B} = -h_{2A} = h_{2B} = 5$ meV

The interaction between each exchange field component is not taken into account in this study to simplify the analysis. The tight-binding Hamiltonians and low-energy effective Hamiltonians [21] are used to describe the electrons transport in this study. In ferromagnetic regions FM1 and FM2, the Hamiltonian is defined as

$$\begin{aligned} H_{FM1} &= v_F(p_x\tau^x - \eta p_y\tau^y) - \Delta_{\eta\sigma 1}\tau^z - \mu_{\sigma 1} \\ H_{FM2} &= v_F(p_x\tau^x - \eta p_y\tau^y) - \Delta_{\eta\sigma 2}\tau^z - \mu_{\sigma 2}. \end{aligned} \quad (1)$$

The k and k' valley is represented with $\eta = +1$ and $\eta = -1$, while spin $\uparrow$ and $\downarrow$ is represented with $\sigma = +1$ and $\sigma = 11$, respectively. The notations $\hat{p}_x = -i\hbar\dfrac{\partial}{\partial x}, \hat{p}_y = -i\hbar\dfrac{\partial}{\partial y}$, and the notations τ^x, τ^y, τ^z are elements of Pauli spin-operators used to represent pseudospin states. $v_F \cong 5.5 \times 10^5$ m/s [22] indicates Fermi velocity near Dirac point. Other parameters in (1) are explained as follows:

$\Delta_{\eta\sigma 1} = \eta\sigma\Delta_{SO} - \Delta_E + \sigma\Delta_{M1}$: Spin-valley dependent energy gaps at FM1 gate
$\Delta_{\eta\sigma 2} = \eta\sigma\Delta_{SO} - \Delta_E + \sigma\Delta_{M2}$:Spin-valley dependent energy gaps at FM2 gate
$\Delta_{SO} = 3.9$ meV : Effective spin-orbit interaction
$\Delta_E = eDE_z$: Electric field-induced energy gap
$\Delta_{M1} = \dfrac{(h_{1A} - h_{1B})}{2}$: Exchange field-induced energy gaps at FM1 gate
$\Delta_{M2} = \dfrac{(h_{2A} - h_{2B})}{2}$: Exchange field-induced energy gaps at FM2 gate
$\mu_{\sigma 1} = \mu + \sigma u_{M1}$: Spin-dependent chemical potentials at FM1 gate
$\mu_{\sigma 2} = \mu + \sigma u_{M2}$: Spin-dependent chemical potentials at FM2 gate
Here, the notations $u_{M1} = (h_{1A} + h_{1B})/2$ and $u_{M2} = (h_{2A} + h_{2B})/2$, since the chemical potential in the barrier is spin-dependent relating to the exchange field. The Hamiltonian in normal regions NM2 with photo irradiation is defined as

$$H_{NM2} = v_F(p_x\tau^x - \eta p_y\tau^y) - \Delta_{\eta\sigma}\tau^z, \quad (2)$$

where the spin-valley dependent energy gap could be expressed with $\Delta_{\eta\sigma} = \eta\sigma\Delta_{SO} + \eta\lambda_\Omega$ and the light irradiation term λ_Ω could be described as

$$\lambda_\Omega = (e\Lambda V_F)^2/\hbar\Omega. \quad (3)$$

We use $\Lambda = eA_0a/\hbar$ which is a dimensionless number to characterize the light intensity with e represents the elementary charge, A_0 represents the magnitude of light wave, and a represents the lattice constant of silicene [12, 15]. The value of is generally less than 1 for the intensity from light sources in the frequency range of our interest [13].

In the normal regions NM1 and NM3 where there is neither photo irradiation nor external electric field, the spin-valley dependent energy gap is $\Delta_{\eta\sigma 3} = \eta\sigma\Delta_{SO}$. Therefore, the Hamiltonian in these two regions could be defined as

$$H_{NM1} = H_{NM3} = v_F(p_x\tau^x - \eta p_y\tau^y) - \eta\sigma\Delta_{so}\tau^z. \quad (4)$$

3. TRANSPORT FORMULAE

In this section, we describe the electrons transport in the device structure. Using the Hamiltonians from (1), (2) and (4), the wave functions in the NM1, FM1, NM2, FM2, and NM3 regions can be defined respectively as

$$\begin{aligned} \Psi_{NM1} &= \left[\begin{pmatrix} 1 \\ A_{\eta\sigma}e^{-i\eta\theta}\end{pmatrix}e^{ik_x x} + r_{\eta\sigma}\begin{pmatrix} 1 \\ -A_{\eta\sigma}e^{i\eta\theta}\end{pmatrix}e^{-ik_x x}\right]e^{ik_{//}y}, \\ \Psi_{FM1} &= \left[a_{\eta\sigma}\begin{pmatrix} 1 \\ B_{\eta\sigma}e^{-i\eta\alpha_1}\end{pmatrix}e^{il_x x} + b_{\eta\sigma}\begin{pmatrix} 1 \\ -B_{\eta\sigma}e^{i\eta\alpha_1}\end{pmatrix}e^{-il_x x}\right]e^{ik_{//}y}, \\ \Psi_{NM2} &= \left[g_{\eta\sigma}\begin{pmatrix} 1 \\ M_{\eta\sigma}e^{-i\eta\beta}\end{pmatrix}e^{im_x x} + f_{\eta\sigma}\begin{pmatrix} 1 \\ -M_{\eta\sigma}e^{i\eta\beta}\end{pmatrix}e^{-im_x x}\right]e^{ik_{//}y}, \\ \Psi_{FM2} &= \left[p_{\eta\sigma}\begin{pmatrix} 1 \\ N_{\eta\sigma}e^{-i\eta\alpha_2}\end{pmatrix}e^{in_x x} + q_{\eta\sigma}\begin{pmatrix} 1 \\ -N_{\eta\sigma}e^{i\eta\alpha_2}\end{pmatrix}e^{-in_x x}\right]e^{ik_{//}y}, \\ \Psi_{NM3} &= \left[t_{\eta\sigma}\begin{pmatrix} 1 \\ A_{\eta\sigma}e^{-i\eta\theta}\end{pmatrix}e^{ik_x x}\right]e^{ik_{//}y}, \end{aligned} \quad (5)$$

where

$$A_{\eta\sigma} = \frac{E + \eta\sigma\Delta_{SO}}{\sqrt{E^2 - \Delta_{SO}^2}}, B_{\eta\sigma} = \frac{E + \mu_{\sigma 1} + \Delta_{\eta\sigma 1}}{\sqrt{(E + \mu_{\sigma 1})^2 - \Delta_{\eta\sigma 1}^2}}.$$

$$M_{\eta\sigma} = \frac{E + \Delta_{\eta\sigma}}{\sqrt{E^2 - \Delta_{\eta\sigma}^2}}, N_{\eta\sigma} = \frac{E + \mu_{\sigma 2} + \Delta_{\eta\sigma 2}}{\sqrt{(E + \mu_{\sigma 2})^2 - \Delta_{\eta\sigma 2}^2}}.$$

The coefficients $r_{\eta\sigma}, a_{\eta\sigma}, b_{\eta\sigma}, g_{\eta\sigma}, f_{\eta\sigma}, p_{\eta\sigma}, q_{\eta\sigma}, t_{\eta\sigma}$ could be obtained by using the following boundary conditions to obtain matrix equation. After that, Cramer's rule might be used to solve that matrix equation.

$$\begin{aligned} &\Psi_{NM1}(0) = \Psi_{FM1}(0), \\ &\Psi_{FM1}(L_G) = \Psi_{NM2}(L_G), \\ &\Psi_{FM1}(L_G + L) = \Psi_{NM2}(L_G + L), \\ &\Psi_{FM2}(2L_G + L) = \Psi_{NM3}(2L_G + L). \end{aligned} \quad (6)$$

Here, the parameters $r_{\eta\sigma}$ and $t_{\eta\sigma}$ represent the reflection and transmission coefficients of electronic waves, respectively. The wave vectors in the x-direction in each region are given by

$$k_x=\frac{\sqrt{E^2-\Delta_{SO}^2}\cos\theta}{\hbar v_F}, l_x=\frac{\sqrt{(E+\mu_{\sigma 1})^2-\Delta_{\eta\sigma 1}^2}\cos\alpha_1}{\hbar v_F},$$

$$m_x=\frac{\sqrt{E^2-\Delta_{\eta\sigma}^2}\cos\beta}{\hbar v_F}, n_x=\frac{\sqrt{(E+\mu_{\sigma 2})^2-\Delta_{\eta\sigma 2}^2}\cos\alpha_2}{\hbar v_F}.$$

The incident angles on each junction can be obtained through the conservation of components in y-direction as given by

$$k_{//}=\frac{\sqrt{E^2-\Delta_{SO}^2}\sin\theta}{\hbar v_F}=\frac{\sqrt{(E+\mu_{\sigma 1})^2-\Delta_{\eta\sigma 1}^2}\sin\alpha_1}{\hbar v_F}$$
$$=\frac{\sqrt{E^2-\Delta_{\eta\sigma}^2}\sin\beta}{\hbar v_F}=\frac{\sqrt{(E+\mu_{\sigma 2})^2-\Delta_{\eta\sigma 2}^2}\sin\alpha_2}{\hbar v_F}.$$

Here, θ is the incident angle of electrons at the NM1/FM1 junction, β is the incident angle at FM1/NM2 junction, α_1 is the incident angle at NM2/FM2 junction, and α_2 is the incident angle at FM2/NM3 junction. The transmission probability amplitude $T_{\eta\sigma}$ is calculated via the formula

$$T_{\eta\sigma}=J_t/J_{in}=|t_{\eta\sigma}|^2, \tag{7}$$

where J_t and J_{in} are current densities of transmitted electrons and injected electrons, respectively.

It is known that spin-polarized conductance and valley-polarized conductance in ballistic regime at zero temperature can be obtained with integration on all incident angles using the standard Landauer's formalism [23, 24] as shown below

$$T_{\eta\sigma}=J_t/J_{in}=|t_{\eta\sigma}|^2 \tag{8}$$

The parameters in (8) are described in details as follows:

$N(E)=\frac{W}{\pi\hbar v_F}\sqrt{E^2-\Delta_{SO}^2}$: Density of state at the transport channel of normal silicene junction

$G_0=\frac{4e^2}{h}N_0(E)$: Unit conductance

$N_0(E)=\frac{W}{\pi\hbar v_F}|E|$: Density of state at transport channel in silicene excluding the spin-orbit interaction effect

h : Planck's constant

W : The width of silicene film

For our numerical analysis in this study, the spin polarization (SP), valley polarization (VP) and tunnelling magnetoresistance (TMR) are defined respectively as follows:

$$SP(\%)=\frac{(G_{k\uparrow}+G_{k'\uparrow})-(G_{k\downarrow}+G_{k'\downarrow})}{G_T}\times 100,$$

$$VP(\%)=\frac{(G_{k\uparrow}+G_{k\downarrow})-(G_{k'\uparrow}+G_{k'\downarrow})}{G_T}\times 100,$$

and
$$TMR(\%)=\frac{G_P-G_{AP}}{G_P}\times 100. \tag{9}$$

From (9), spin polarization could be considered as the difference between spin-up components and spin-down components divided by total conductance. In the same manner, valley polarization could be considered as the difference between k-valley components and k'-valley components divided by total conductance. On the other hand, tunnelling magnetoresistance could be considered as the difference between conductance in P-junction (G_P) and AP-junction (G_{AP}) normalized by the conductance in P-junction. Here, the total conductance G_T is defined as

$$G_T=G_{k\uparrow}+G_{k\downarrow}+G_{k'\uparrow}+G_{k'\downarrow}. \tag{10}$$

4. RESULTS AND DISCUSSION

In this study, we set the device structure parameters to be $L=25$ nm and $L_G=25$ nm, and electrons excited energy to be $E=4$ meV. Fig. 2 compares the normalized conductance when there is no electric fields on the ferromagnetic gates under different exchange field configurations and light irradiation conditions. Fig. 2(a) shows conductance in P junction when there is no light irradiation. It depicts complete spin- and valley-polarization, which is useful for applications in spin-valley filtering devices. When the same P junction is irradiated with 2000 THz light, the spin-valley polarizations particularly the spin-up currents ($G_{k\uparrow}$ and $G_{k'\uparrow}$) are affected to become broader as shown in Fig. 2(b). Fig. 2(c) and (d) show conductance when the irradiated light frequency is varied in P junction and AP junction, respectively. Complete spin-valley polarization can be seen in both figures. In term of applications, Fig. 2(d) in particular shows filtering of $G_{k\uparrow}$ with other spin-valley polarization components being suppressed, which indicates a potential for spin-valley filtering with a certain polarized-photon frequency. Another noteworthy point here is the very small normalized conductance magnitude of less than 0.03. This is due to the fact that in this study the energy $E=4$ meV approaches $\Delta_{SO}=3.9$ meV, which is in the energy range we are interested in due to the intriguing properties near the Dirac cone. As the results, there are fewer density of states available in transport channel and causes lower conductance.

Fig. 3(a) and (b) show spin polarization (SP) with varied electric field E_Z at the ferromagnetic gates when there is no light irradiation in P junction and AP junction, respectively. The comparison of results indicates the effect of exchange field configuration on

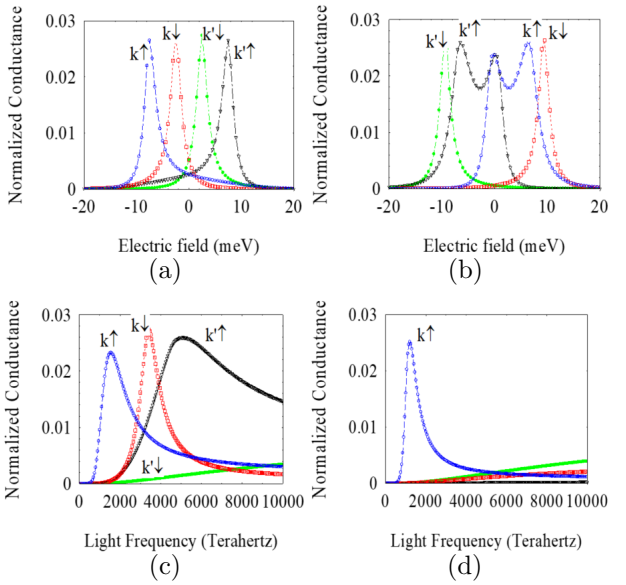

Fig.2: *Normalized conductance when there is (a) no light in P junction, (b) light irradiation at 2000 THz in P junction, (c) light irradiation with varied frequency in P junction, (d) light irradiation with varied frequency in AP junction.*

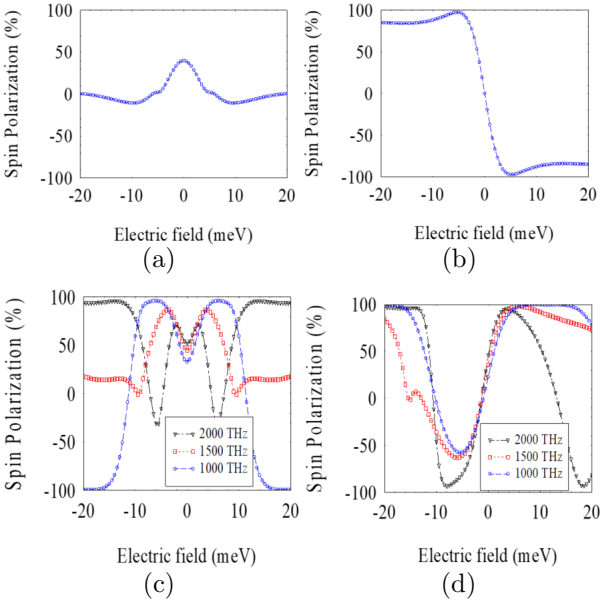

Fig.3: *Spin polarization when there is (a) no light in P junction, (b) no light in AP junction, (c) light irradiation in P junction, (d) light irradiation in AP junction.*

the spin polarization with full switching from +100% to −100% at electric field around 0 meV in AP junction. Fig. 3(c) and (d) show spin polarization characteristics when light with frequency of 1000 THz, 1500 THz and 2000 THz are irradiated to P junction and AP junction, respectively. They clearly depict the effect of light irradiation in both exchange field configurations. Particularly in P junction, the range of spin polarization is enhanced as illustrated in Fig. 3(c). The spin polarization shows switching from −100% to +100% in negative electric field, and from +100% to −100% in positive electric field when the frequency is 1000 THz. On the other hand, oscillation can be observed in AP junction as shown in Fig. 3(d), particularly when the frequency is 2000 THz.

The effects of light irradiation on valley polarization (VP) characteristics are shown in Fig. 4. The first two figures, Fig. 4(a) and (b), are the cases without light irradiation in P junction and AP junction, where it is clear that the exchange field configuration contributes to the characteristics of valley polarization. However, in the opposite to spin polarization where the full switching occurred in AP junction as shown in Fig. 3(b), the valley polarization indicates full switching from +100% to −100% at the electric field around 0 meV in P junction as depicted in Fig. 4(a). Fig. 4(c) and (d) show valley polarization when 1000 THz, 1500 THz and 2000 THz light are irradiated to P junction and AP junction, respectively.

It is interesting to see that both P junction and AP junction show similar characteristics with photo irradiation. Moreover, neither exchange field nor light frequency in the off-resonant region which is the range of our investigation has significant impact on the valley polarization characteristics. In both P and AP junction, the valley polarization shows sharp full switching from −100% to +100%, particularly in P junction. These results might be useful for applications in valleytronics.

Tunnelling magnetoresistance (TMR) is an interesting phenomenon which is widely applied to many types of devices such as read heads of hard disk drive, magnetoresistive random-access memory (MRAM), and sensing applications. Our study shows that photo irradiation also affects TMR characteristics as illustrated in Fig. 5(b) where light with frequency of 1000 THz, 1500 THz and 2000 THz are irradiated comparing to Fig. 5(a) where there is no light irradiation. It shows that in all three light frequencies, the amplitude of TMR increases significantly with photo irradiation. Overall, the changes of electron transport characteristics as seen in SP, VP, and TMR after circularly polarized photo irradiation from Fig. 3 to Fig. 5 is considered to be the results of photon dressing effect, which can modify the band structure and change electronic properties of the materials [12, 13]. Photon dressing is the interaction between photons and electrons in nanoscale, which causes a new phase of electronic structure [25]. The interaction results in quasiparticles of combined photons and electrons with a distinct Floquet-Bloch band structure [26]. When light with off-resonant frequency is irradiated to a matter, the light energy would not be absorbed

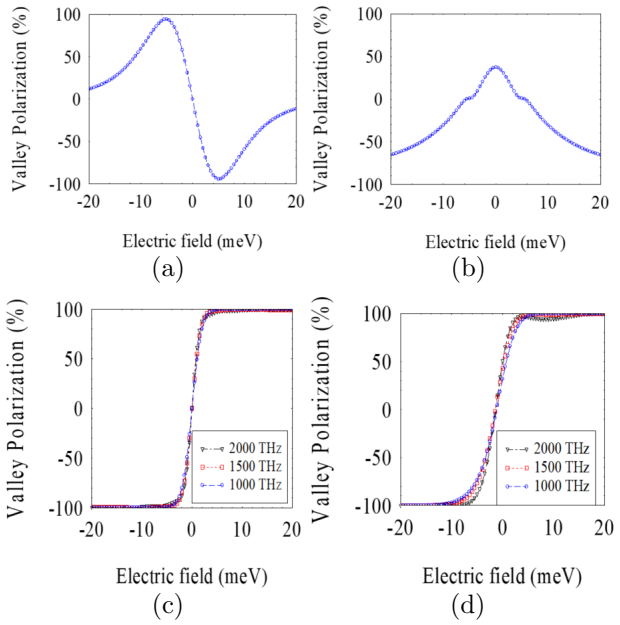

Fig.4: *Valley polarization when there is (a) no light in P junction, (b) no light in AP junction, (c) light irradiation in P junction, (d) light irradiation in AP junction.*

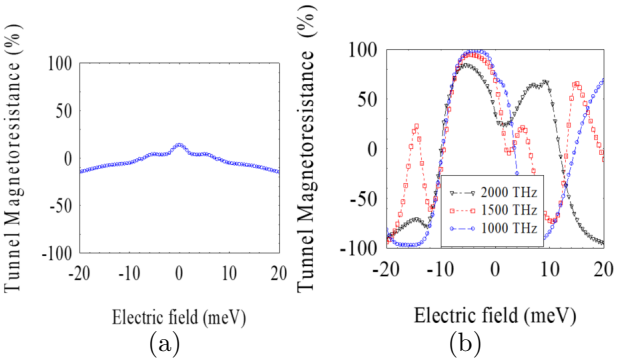

Fig.5: *Tunnelling magnetoresistance when there is (a) no light, (b) circularly polarized light irradiation.*

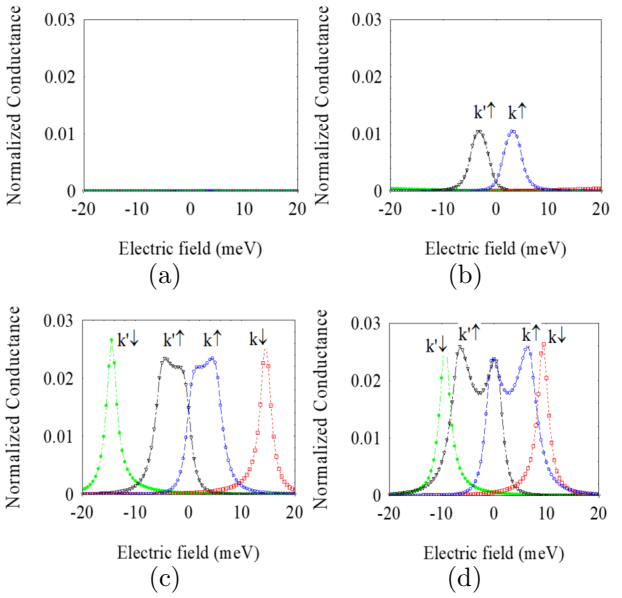

Fig.6: *Normalized conductance when the irradiated light frequency is (a) 500 THz, (b) 1000 THz, (c) 1500 THz, (d) 2000 THz.*

by electronic states of the matter. The photon energy instead dresses the electronic states via virtual photon processes. Because electronic states are affected or dressed by the photon, we call this interaction photon dressing, which gives rise to new electronic states with different properties.

We have also investigated the parameters that play an important role on light irradiation effects, where we particularly pay attention to light frequency and light intensity. Fig. 6 compares the normalized conductance in P junction when there is no electric fields under the irradiation of different light frequency. Fig. 6(a) shows the insulating states when the light frequency is low at 500 THz comparing to the complete spin- and valley-polarization when there is no light irradiation in Fig. 2(a). This is considered to be the results from altered band structure due to photon dressing effect, which in turn reduces the transmission probability of electrons in the junction. Fig. 6(b) and (c) show the increasing conductance along with higher light frequency, and Fig. 6(d) illustrates the same conductance characteristics as shown in Fig. 2(b) when light frequency is 2000 THz.

Next we look at the effects of light intensity on tunnelling magnetoresistance due to its simpler characteristics comparing to those of conductance, which makes it is easier to analyse. Fig. 7(a) and (b) illustrate the tunnelling magnetoresistance characteristics with different light frequency when the light intensity parameter Λ is 0.03 and 0.1, respectively. It is obvious to see that the tunnelling magnetoresistance is bigger in Fig. 7(b) where Λ is 0.1 than in Fig. 7(a) where Λ is 0.03. Furthermore, the tunnelling magnetoresistance is even bigger in Fig. 5(b), where Λ is 0.3, than in Fig. 7(b). When we compare the similar TMR characteristics in Fig. 5(a) and Fig. 7(a), it might be possible to say that when the light intensity is lower, the effect of light irradiation is weaker and gets closer to the state when there is no light irradiation. The results show that light intensity is the parameter that plays a significant role to trigger light irradiation effects.

The conductance, spin polarization, valley polarization, and tunelling magnetoresistance of the structure could be explained with the energy band structure of each region as shown in Fig. 8. Since the band gap at the ferromagnetic barrier is determined by spin-valley dependent energy gap $\Delta_{\eta\sigma} = \eta\sigma\Delta_{SO} - \Delta_E + \sigma\Delta_M$, the band gap for each spin-valley component is different among each other. For

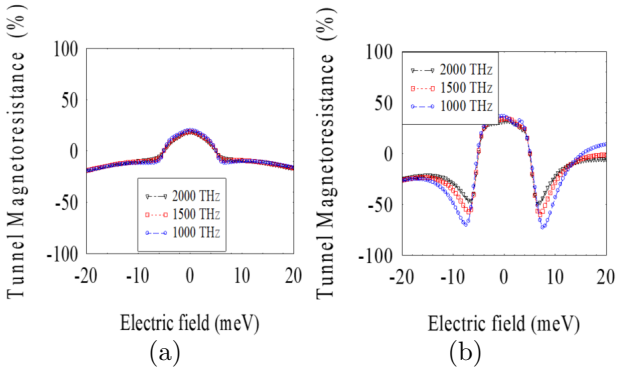

Fig.7: *Tunnelling magnetoresistance when the irradiated light intensity parameter (a) Λ is 0.03, (b) Λ is 0.1.*

instance, the spin-valley index of $k\uparrow$ is $\eta = +1$, $\sigma = +1$. In the same manner, the spin-valley index of $k'\uparrow$ is $\eta = -1$, $\sigma = +1$, $k\downarrow$ is $\eta = +1$, $\sigma = -1$ and $k'\downarrow$ is $\eta = -1$, $\sigma = -1$. Therefore, the spin-valley dependent energy gap for each spin-valley current component is

$$\begin{aligned}
\Delta_{k\uparrow} &= \Delta_{SO} - \Delta_E + \Delta_M, \\
\Delta_{k'\uparrow} &= -\Delta_{SO} - \Delta_E + \Delta_M, \\
\Delta_{k\downarrow} &= -\Delta_{SO} - \Delta_E - \Delta_M, \\
\Delta_{k'\downarrow} &= \Delta_{SO} - \Delta_E - \Delta_M.
\end{aligned} \tag{11}$$

On the other hand, the energy band gap at the normal region NM2 with light irradiation is determined by another spin-valley dependent energy gap $\Delta_{\eta\sigma} = \eta\sigma\Delta_{SO} + \eta\lambda_\Omega$. This energy gap also has different impact to each spin-polarized and valley-polarized current components. In short, the contributions from electric-field-induced energy gap Δ_E, exchange-field-induced energy gap Δ_M, and spin-orbit coupling Δ_{SO} cause changes on the energy band gap. Furthermore, the spin-dependent chemical potential $\mu_\sigma = \mu + \sigma u_M$ and the middle gate potential U/e also affect the low-energy Hamiltonian and wave functions as described in Section II Model. Hence, they also affect the Fermi level and energy band structure of the junction. Since each spin-valley component might experience the energy band structure differently, the transmission probability amplitude of each spin-valley component could be different. As the results, conductance, spin polarization, valley polarization, and tunelling magnetoresistance of each spin-valley component might be different.

The results from this theoretical study are based on tight-binding model, which is a widely accepted methodology in the research community. One of the reasons for the popularity is its simplicity and efficiency [27-29]. The accuracy of the tight-binding approximation has increased over the time, such as the inclusion of total-energy calculations and density

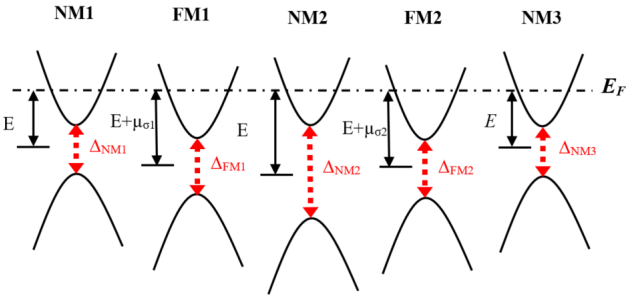

Fig.8: *Band structure in each regions of the device structure.*

functional approach [30, 31]. Although it is impossible to directly compare the theoretical results with the those from experiments due to the technical challenges facing the realization of free-standing silicene, it has been found that the properties of silicene from tight-binding model is comparable to those from more accurate density functional theory (DFT) [32]. There have been several studies discussing the accuracy and effectiveness of tight-binding approximation elemental 2D materials such as graphene and silicene [33, 34]. The results from our study may be used as a guideline for device applications in the future.

5. SUMMARY AND CONCLUSION

We have studied the impact of off-resonant circularly polarized photo irradiation on the spin-polarized and valley-polarized transport in a double ferromagnetic-gate silicene-based junction. We found that all components of the polarized spin and valley currents ($k\uparrow, k\downarrow, k'\uparrow, k'\downarrow$) are affected by the light irradiation. The irradiation of off-resonant circularly polarized light on silicene modifies the energy band structure and changes electronic properties, probably due to the photon dressing effect. Photo irradiation also has strong impact on tunneling magnetoresistances. For the silicene junction in our study, we found that the range of spin polarization was enhanced in P junction, and discovered the oscillation of spin polarization in AP junction. The investigation results show that the valley polarization is affected in different way from spin polarization. Both P junction and AP junction show similar valley polarization characteristics with photo irradiation, and neither exchange field configuration nor light frequency has significant impact on the valley polarization. The effect of photo irradiation on tunneling magnetoresistances is also non-trivial with the tunneling magnetoresistance amplitude increases significantly comparing to when there is no light irradiation. We discovered that the light intensity plays the major role to trigger the photo irradiation effect, with low light intensity causes similar characteristics to when there is no light irradiation. On the other hand, the light frequency affects the characteristics in different way

causing no electronic transmission at all when the frequency is low. In summary, we demonstrate the impact of off-resonant circularly polarized photo irradiation on polarized spin and valley transport in a double ferromagnetic-gate silicene-based junction. This might be useful for future applications in spintronics and valleytronics, such as photo sensing devices. Analysis of the light frequency effect found the possibility to filter specific spin-polarized current and valley-polarized current component with appropriate adjustment on the exchange field configuration and electric field direction.

ACKNOWLEDGEMENT

We would like to thank Dr. Bumned Soodchomshom for his fruitful discussions.

References

[1] P. Vogt et al., "Silicene: Compelling Experimental Evidence for Graphenelike Two-Dimensional Silicon," *Physical Review Letters*, Vol. 108, pp. 155501, 2012.

[2] M. Ezawa, "Valley-Polarized Metals and Quantum Anomalous Hall Effect in Silicene," *Physical Review Letters*, Vol. 109, pp. 055502, 2012.

[3] T. Yokoyama, "Spin and Valley Transports in Junctions of Dirac Fermions," *New Journal of Physics*, Vol. 16, pp. 085005, 2014.

[4] T. Yokoyama, "Controllable Valley and Spin Transport in Ferromagnetic Silicene Junctions," *Physical Review B*, Vol. 87, pp. 241409(R), 2013.

[5] V. Vargiamidis and P. Vasilopoulos, "Electric- and Exchange-Field Controlled Transport through Silicene Barriers: Conductance Gap and Near-Perfect Spin Polarization," *Applied Physics Letters*, Vol. 105, pp. 223105, 2014.

[6] B. Soodchomshom, "Perfect Spin-Valley Filter Controlled by Electric Field in Ferromagnetic Silicene," *Journal of Applied Physics*, Vol. 115, pp. 023706, 2014.

[7] X.Q. Wu and H. Meng, "Gate-Tunable Valley-Spin Filtering in Silicene with Magnetic Barrier," *Journal of Applied Physics*, Vol. 117, pp. 203903, 2015.

[8] W. F. Tsai, et al., "Gated Silicene as a Tunable Source of Nearly 100% Spin-Polarized Electrons," *Nature Communications*, Vol. 4, pp. 1500, 2013.

[9] Y. Wang and Y. Lou, "Controllable Spin Transport in Dual-Gated Silicene," *Physics Letters A*, Vol. 378, pp. 2627, 2014.

[10] P. Chantngarm, K. Yamada, and B. Soodchomshom, "Lattice-Pseudospin and Spin-Valley Polarizations in Dual Ferromagnetic-Gated Silicene Junction," *Superlattices and Microstructures*, Vol. 94, pp. 13-24, 2016.

[11] L. Tao, et al., "Silicene Field-Effect Transistors Operating at Room Temperature," *Nature Nanotechnology*, Vol. 10, pp. 227-231, 2015.

[12] T. Kitagawa et al., "Transport Properties of Nonequilibrium Systems under the Application of Light: Photoinduced Quantum Hall Insulators without Landau Levels," *Physical Review B: Condensed Matter and Materials Physics*, Vol. 84, pp. 235108, 2011.

[13] M. Ezawa, "Photoinduced Topological Phase Transition and a Single Dirac-Cone State in Silicene," *Physical Review Letters*, Vol. 110, pp. 026603, 2013.

[14] Y. Mohammadi and B. A. Nia, "Controllable Photo-Induced Spin and Valley Filtering in Silicene," *Superlattices and Microstructures*, Vol. 96, pp. 259-266, 2016.

[15] L. B. Ho and T. N. Lan, "Photoenhanced Spin/Valley Polarization and Tunneling Magnetoresistance in Ferromagnetic-Normal-Ferromagnetic Silicene Junction," *Journal of Physics D: Applied Physics*, Vol. 49, pp. 375106, 2016.

[16] P. Chantngarm, K. Yamada, and B. Soodchomshom, "Polarized-Photon Frequency Filter in Double-Ferromagnetic Barrier Silicene Junction," *The Journal of Magnetism and Magnetic Materials*, Vol. 429, pp. 16-22, 2017.

[17] H. Haugen, D. Huertas-Hernando, and A. Brataas, "Spin Transport in Proximity-Induced Ferromagnetic Graphene," *Physical Review B: Condensed Matter and Materials Physics*, Vol. 77, pp. 115406, 2008.

[18] W. Happer and B. S. Mathur, "Off-Resonant Light as a Probe of Optically Pumped Alkali Vapors," *Physical Review Letters*, Vol. 18, pp. 577-580, 1967.

[19] M. Auzinsh, D. Budker, S. M. Rochester, *Optically polarized atoms: Understanding light-atom interactions*, Oxford University Press, 2010.

[20] M. Ezawa, "Topological Phase Transition and Electrically Tunable Diamagnetism in Silicene," *The European Physical Journal B*, Vol. 85, pp. 363, 2012.

[21] M. Ezawa, "Spin Valleytronics in Silicene: Quantum Spin Hall-Quantum Anomalous Hall Insulators and Single-Valley Semimetals," *Physical Review B: Condensed Matter and Materials Physics*, Vol. 87, pp. 155415, 2013.

[22] C. C. Liu, W. Feng, and Y. Yao, "Quantum Spin Hall Effect in Silicene and Two-Dimensional Germanium," *Physical Review Letters*, Vol. 107, pp. 076802, 2011.

[23] K. S. Novoselov, et al., "Two-Dimensional Gas of Massless Dirac Fermions in Graphene," *Nature*, Vol. 438, pp. 197, 2005.

[24] R. Landauer, "Spatial Variation of Currents and Fields Due to Localized Scatterers in Metallic

Conduction," *IBM Journal of Research and Development*, Vol. 1, pp. 223-231, 1957.

[25] U. D. Giovannini, H. Hubener, and A. Rubio, "Monitoring Electron-Photon Dressing in WSe2," *Nano Letters*, Vol. 16, pp. 7993-7998, 2016.

[26] F. H. M. Faisal and J. Z. Kaminski, "Floquet-Bloch Theory of High-Harmonic Generation in Periodic Structures," *Physical Review A*, Vol. 56, pp. 748-762, 1997.

[27] J. C. Slater and G. F. Koster, "Simplified LCAO Method for the Periodic Potential Problem," *Physical Review*, Vol. 94, pp. 1498-1524, 1954.

[28] W. A. Harrison, *Electronic Structure and the Properties of Solids: The Physics of the Chemical Bond*, Dover Publications, 1989.

[29] M. Finnis, *Interatomic Forces in Condensed Matter*, Oxford University Press, 2010.

[30] D. A. Papaconstantopoulos and M. J. Mehl, "The Slater-Koster Tight-Binding Method: A Computationally Efficient and Accurate Approach," *Journal of Physics: Condensed Matter*, Vol. 15, pp. R413-R440, 2003.

[31] M. Elstner, et al., "Self-Consistent-Charge Density-Functional Tight-Binding Method for Simulations of Complex Materials Properties," *Physical Review B*, Vol. 58, pp. 7260-7268, 1998.

[32] C. C. Liu, H. Jiang, and Y. Yao, "Low-energy Effective Hamiltonian Involving Spin-Orbit Coupling in Silicene and Two-Dimensional Germanium and Tin," *Physical Review B*, Vol. 84, pp. 195430, 2011.

[33] L. A. Agapito, et al., "Accurate Tight-Binding Hamiltonians for Two-Dimensional and Layered Materials," *Physical Review B*, Vol. 93, pp. 125137, 2016.

[34] R. Cote and M. Barrette, "Validity of the Two-Component Model of Bilayer and Trilayer Graphene in a Magnetic Field," *Physical Review B*, Vol. 88, pp. 245445, 2013.

Peerasak Chantngarm was born in Bangkok, Thailand. He received B.S. degree in Physics from Kyoto University in Japan. He then received M.S. degree in Computer Engineering from North Carolina State University in USA and PhD degree from Gunma University in Japan. He worked as an IC design engineer at Texas Instruments in Dallas, USA. He also worked as a lecturer at King Mongkut's Institute of Technology Ladkrabang before joining Rajamangala University of Technology Krungthep in Thailand, where he is currently an Associate Professor in Department of Electronics and Telecommunication Engineering. He also worked shortly as a JSPS researcher at the University of Tokyo and as a visiting scholar at Osaka University in Japan. His current research interests are in spintronics, density functional theory, and quantum computation.

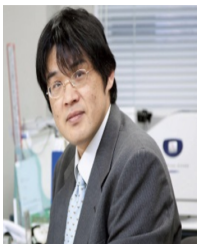

Kou Yamada was born in Akita, Japan, in 1964. He received B.S. and M.S. degrees from Yamagata University, Yamagata, Japan, in 1987 and 1989, respectively, and the Dr. Eng. degree from Osaka University, Osaka, Japan in 1997. From 1991 to 2000, he was with the Department of Electrical and Information Engineering, Yamagata University, Yamagata, Japan, as a research associate. From 2000 to 2008, he was an associate professor in the Department of Mechanical System Engineering, Gunma University, Gunma, Japan. Since 2008, he has been a professor in the Department of Mechanical System Engineering, Gunma University, Gunma, Japan. His research interests include robust control, repetitive control, process control and control theory for inverse systems and infinite-dimensional systems. Dr. Yamada received the 2005 Yokoyama Award in Science and Technology, the 2005 Electrical Engineering/Electronics, Computer, Telecommunication, and Information Technology International Conference (ECTI-CON 2005) Best Paper Award, the Japanese Ergonomics Society Encouragement Award for Academic Paper in 2007, the 2008 Electrical Engineering/Electronics, Computer, Telecommunication, and Information Technology International Conference (ECTI-CON 2008) Best Paper Award and Fourth International Conference on Innovative Computing, Information and Control Best Paper Award in 2009.